Comprehensive calculations of 4p and 4d lifetimes for the Cu sequence

Lorenzo J. Curtis and Constantine E. Theodosiou
Department of Physics and Astronomy, The University of Toledo, Toledo, Ohio 43606
(Received 29 July 1988)

Computed lifetimes for the $4p\ ^2P_{1/2}$, $4p\ ^2P_{3/2}$, $4d\ ^2D_{3/2}$, and $4d\ ^2D_{5/2}$ levels in the copper isoelectronic sequence are presented for atomic numbers $Z=29-92$. These calculations agree well with recent high-precision lifetime measurements, conflict with the isoelectronic trend of single-configuration Dirac-Fock calculations, and agree at lower Z with the multiplet values of multiconfiguration Hartree-Fock calculations using experimental transition energies. Our calculations involve the inclusion of experimental energy-level data and the use of a Hartree-Slater potential to represent the ionic core. It is found that the core-polarization effects are significant and must be included to obtain agreement with experiment, at least for the lower members of the isoelectronic sequence. As part of the study, we have combined semiempirical parametrizations of the existing database with Dirac-Fock calculations to produce a set of values for the ionization potentials and the 4p and 4d excitation energies for all stable ions in this sequence.

I. INTRODUCTION

Ions in the 29-electron copper isoelectronic sequence have been extensively studied both theoretically and experimentally, because of their deceivingly simple electronic structure and their applications as sources of reference lines in spectroscopy. In addition, they serve as impurity concentration indicators in high-temperature plasmas. Although these systems consist basically of a single electron outside closed shells, their theoretical treatment is especially complicated in the lower members of the sequence by strong mixing with core-excited configurations, which not only shift the position of the 4s and 4p levels but also alter their spectroscopic character.

The experimental determination of the lifetimes and oscillator strengths of the principal series of the Cu sequence generally requires nonselective excitation, and is plagued by strong cascade contributions. For this reason, multiexponential fits of the measured decay curves are not normally dependable.[1,2] Presently, the only dependable method of lifetime determination for these levels involves the joint analysis of cascade-related arbitrarily normalized decay curves, or ANDC method.[3-7] Theoretically, core polarization and other types of electron correlation, spin-orbit coupling and other relativistic interactions, and the advantages of Breit-Pauli and fully relativistic treatments can vary with the degree of ionicity, and the applicability of various *ab initio* approaches changes over the sequence.

Elaborate theoretical calculations have been published,[8-14] high-precision measurements using the ANDC method have recently been reported for the 4s-4p transitions in the Cu isoelectronic sequence,[15-22] and discrepancies have emerged. It is the purpose of this paper to report new calculations that reproduce the observed lifetimes to within experimental accuracies and provide precise predictions for higher members of the sequence. These computations utilize the Hartree-Slater method to calculate a realistic potential that describes the interaction of the electron with the ionic core and incorporate the effects of spin-orbit interaction and especially of core polarization. In order to extend the application of this method, we have also used semiempirical parametrizations of the spectroscopic data and multiconfiguration Dirac-Fock (MCDF) calculations to produce a set of values for the ionization potentials and the 4p and 4d excitation energies for all stable ions in the Cu sequence.

II. SURVEY OF PRECISION EXPERIMENTAL LIFETIME DATA

A compilation of lifetime data for 4p lifetimes in the Cu sequence must be made critically, because early measurements based solely on exponential curve fitting systematically overestimated the lifetimes. Analyses that fit a sum of exponential functions to the decay curve of a heavily cascaded alkalilike resonance transition almost invariably overestimate the lifetime,[1,2] and such data should be categorically excluded from comparisons with theory.

The only source of direct lifetime measurements for highly ionized atomic systems is by foil excitation of a fast ion beam, which is non-state-selective. Since these intrashell decay channels are repopulated by faster extrashell cascades and by the yrast chain, experimental decay curves exhibit both growing-in and growing-out cascades, which mask the primary lifetime. However, precision beam-foil measurements can be made that properly account for cascade repopulation and provide internal tests that insure that quoted uncertainties (nominally 5%) are realistic. The ANDC method[3,4] exploits dynamical correlations among cascade-related decay curves to reliably extract lifetimes. For alkalilike resonance transitions, cascading occurs dominantly along the yrast chain, and can often be accounted for using only a single repopulation channel. Very rugged algorithms have been developed[5,6] that permit reliable lifetimes to be extracted, even in cases where the cascade contributions are dom-

inant and studies of the propagation and correlation of errors have been made.[7]

A series of beam-foil lifetime measurements for ions in the Cu sequence employing the ANDC method have recently been reported,[15–22] which comprise a database against which theoretical calculations should be compared. The measurements have been performed on the individual fine-structure levels to typically 5% accuracies, and include the ions Zn II (Ref. 15), Ga III (Ref. 16), Ge IV (Ref. 17), As V (Ref. 18), Se VI (Ref. 19), Kr VIII (Refs. 20 and 21), and I XXV (Ref. 22). These experimental lifetimes and their quoted uncertainties will be given in Table IV and their isoelectronic trend will be described in Sec. IV and Fig. 3. In addition, a beam-foil measurement in Mo XIV (Ref. 23) which used population simulations to account for cascades as an alternative to the ANDC method, a Hanle effect measurement of Zn II (Ref. 24), and a value for Cu I based on a critical evaluation[25] of the existing data will also be included in Table IV. Other earlier measurements which utilized only curve-fitting methods or determined only multiplet values (cf. bibliographic citations in Refs. 2 and 15–25) contain systematic errors which exceed quoted uncertainties, and should not be included in modern comparisons with theory.

III. THEORETICAL FORMULATION

Several types of transition-probability calculations have been made for this sequence, but each suffers from limitations. *Ab initio* Dirac-Fock calculations[8,9] treat the fine structure of $4p$ levels in a fully relativistic manner, which is very important for high stages of ionization. However, these calculations do not adequately describe correlation effects, and show large disagreements with experiment. Nonrelativistic multiconfiguration Hartree-Fock calculations have been made[10] which include electron correlation corrections. However, the lifetime results obtained in this manner are not truly *ab initio* since only a single value for the line strength is obtained for both $4p$ levels, and the experimental wavelengths must be used to obtain level lifetimes. Semiempirical calculations, using the Coulomb approximation, have also been performed,[14] but the applicability of this method has been limited by the availability of measured spectroscopic data as input, and by ambiguities in the choice of the inner cutoff.

A possible criterion for selecting between a fully relativistic treatment without electron correlation and a nonrelativistic treatment with correlation is illustrated in Fig. 1. Here relativistic theoretical values for the ratio of the line strengths $S(\frac{1}{2},\frac{3}{2})/S(\frac{1}{2},\frac{1}{2})$ for the fine-structure transitions are plotted versus the nuclear charge Z. In a nonrelativistic calculation, this ratio would be exactly 2 (the ratio of the predicted lifetimes is usually adjusted to be proportional to the cube of the ratio of the measured wavelengths). As shown in Fig. 1, this is nearly true for low Z, and the deviation from 2 is less than 1% for elements up to Mo XIV. For higher Z the deviation continues to increase, and (neglecting effects of correlation) exceeds 5% for $Z > 80$.

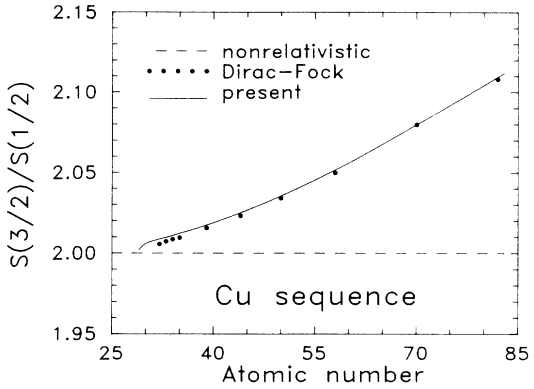

FIG. 1. Plot of the ratio of theoretical line strengths vs nuclear charge for the $4s$-$4p$ fine-structure transitions in the Cu isoelectronic sequence. The solid line denotes the Hartree-Slater calculations reported here and the solid circles the MCDF calculations of Cheng and Kim (Ref. 8).

The approach employed in this work was detailed in Ref. 26 and reviewed more recently in Ref. 27. To summarize, we first establish the effective potential $V_{nlj}(r)$ that the active electron nlj experiences. This potential is taken to consist of a single-electron central field V_c (taken equal to the self-consistent Hartree-Slater approximation prediction $V_{\rm HS}$), a polarization potential V_p (see Ref. 27), plus the spin-orbit interaction term $V_{\rm so}(r)$, i.e.,

$$V_{nlj}(r)=V_{\rm HS}(r)+V_p(r)+V_{\rm so}(r)\ . \tag{1}$$

After establishing the potential we employ the experimental energy level values and integrate Schrödinger's equation

$$\frac{d^2P_{nlj}}{dr^2}=\left[V_{nlj}(r)+\frac{l(l+1)}{r^2}-E_{nlj}\right]P_{nlj}(r) \tag{2}$$

inwards with the correct boundary condition at infinity.[26,28] The inward integration is matched with the outward at the *inner* classical turning point, i.e., near the origin. Since we use a fairly accurate atomic or ionic potential the wave functions so obtained are accurate also at and near the origin. The energy $E=E_{nlj}$ is an input quantity and no iterative procedure is implemented in the solution of the wave equation. Effects of the spin-orbit interaction are included in the treatment implicitly through the experimental energies employed, which depend on it directly, and explicitly through the potential term $V_{\rm so}$.

The effects of core polarization by the valence electron are also included through the modification of the dipole matrix element by the replacement[29,30]

$$\langle f|r|i\rangle \rightarrow \langle f|r(1-\alpha_d\{1-\exp[-(r/r_c)^3]\}/r^3)|i\rangle\ , \tag{3}$$

where α_d is the dipole polarizability of the nickel-like core. The effective cutoff radius r_c is taken equal to the core radius predicted by the Hartree-Slater approximation. The polarization potential, with leading term $1/r^4$, has a small effect on the wave function. However, the

change in the dipole operator [Eq. (3)] was found to be significant.

IV. SPECTROSCOPY DATABASE

The Hartree-Slater theoretical approach[26,27] that we have used involves the integration of the Schrödinger equation with the potential obtained for the ground state of the ion-atom. It is necessary to input values both for the excitation energies of the levels in question and for the ionization limit.

Spectroscopic analysis of the $n=4$ shell and the specification of the ionization potential is now complete[21,31–48] for 32 of the 46 ions in the Cu isoelectronic sequence up to W^{45+}. In addition, measurements[22,49,50] for individual 4*s*-4*p* and 4*p*-4*d* transition wavelengths are available for seven additional ions, I^{24+}, Eu^{34+}, Au^{50+}, Pb^{53+}, Bi^{54+}, Th^{61+}, and U^{63+}. These wavelength measurements permit the specification of excitation energies for the $4p\ ^2P_{3/2}$ level for all seven of these ions, and for the $4d\ ^2D_{5/2}$ level for the six ions below U^{63+}. We have used this total database, together with *ab initio* Dirac-Fock calculations, quantum defect reductions, and screening parameter systematizations, to produce a set of 4*s*, 4*p*, and 4*d* binding energies extending over the entire Cu sequence.

Since binding energies rather than excitation energies are required for our transition probability calculations, accurate estimates for ionization potentials are required over the entire sequence. To obtain these quantities, we performed single-configuration Dirac-Fock calculations[51] of energies for the nickel-like core, both with and without an additional 4*s* electron, for those values of Z for which partial or complete Cu sequence data exist. The computed binding energies of the 4*s* electron were then subtracted from the measured ionization potentials, and this residue was interpolated, extrapolated, and utilized to obtain empirically corrected theoretical estimates of the ionization potentials for the seven ions for which only partial spectroscopic data are available.

Using the measured data supplemented by the seven computed ionization potentials, the Rydberg formula was used to reduce the 4*s*, 4*p*, and 4*d* binding energies to effective quantum defects $\mu = n - n^*$. The quantum defects have a very slow and regular isoelectronic variation, which permits accurate interpolation. Reduction to the quantum-defect formulation has the disadvantage of introducing the large uncertainties inherent in the ionization potentials into the specification of the excited levels, but it was found that the slow variation of the quantum defects more than compensated for this. In quantum-defect space accuracies could be improved by polynomial fitting over a large block of data, whereas for the rapidly varying excitation energies, a moving *local* interpolation would have been necessary.

It was necessary to perform a quantum-defect formulation for only one fine-structure level of each term, because the fine-structure intervals of the $4p\ ^2P$ and $4d\ ^2D$ levels have already been studied in detail.[52,53] Based on a screening parametrization of the Sommerfeld-Dirac formula, precise estimates of these splittings have been published[52,53] that extend over the entire sequence. This is

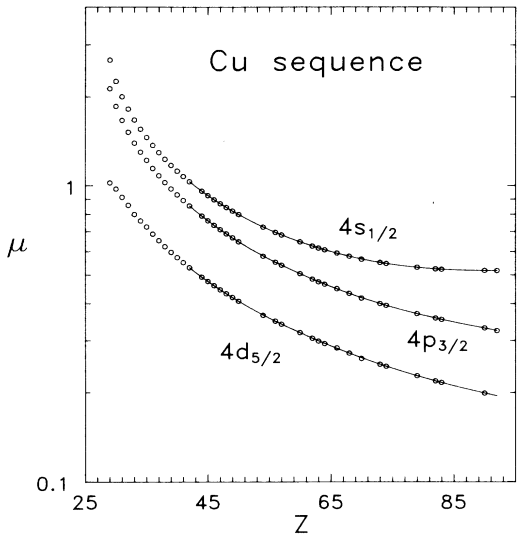

FIG. 2. Plot of the experimental and interpolated values of the quantum defect μ for the $4s_{1/2}$, $4p_{3/2}$, and $4d_{5/2}$ levels of the Cu isoelectronic sequence.

fortunate, since within a multiplet the fine-structure line of higher J is more heavily populated, and its wavelength is generally measured more accurately and over a wider range of ions than the line of lower J. Accordingly, measurements exist for the excitation energy of the $4p\ ^2P_{3/2}$

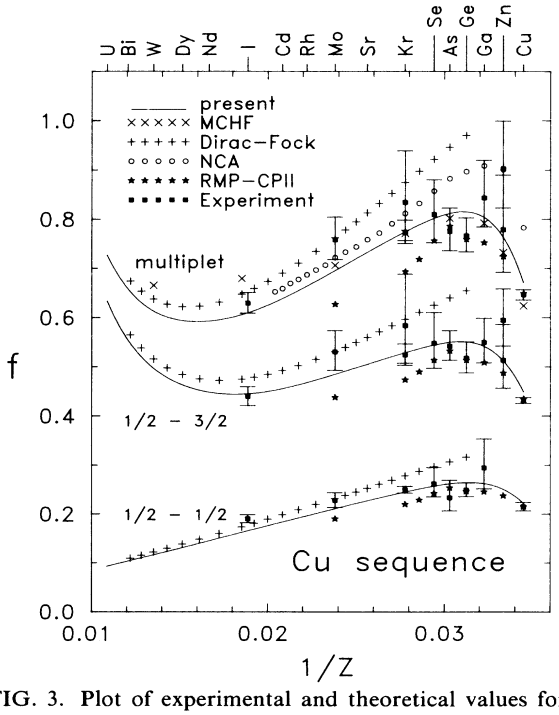

FIG. 3. Plot of experimental and theoretical values for the line and multiplet absorption oscillator strengths vs reciprocal nuclear charge. Solid lines trace the calculations reported here, + denotes the MCDF calculations of Cheng and Kim (Ref. 8), * denotes the calculation of Migdalek and Baylis (Ref. 12), × denotes the MCHF multiplet calculations of Froese Fischer (Ref. 10), and the error bars span the experimental measurements of Refs. 12–22 (which become asymmetric when transformed to *f*-value space).

TABLE I. Compilation of excitation energies (in cm^{-1}), ionization potentials (IP) (in cm^{-1}), and dipole polarizabilities (in a_0^3) for the complete Cu isoelectronic sequence. Quantities in parentheses were obtained by interpolation using three approaches: a fit of $\ln\mu$ to a fifth-order polynomial in ζ to specify the $4s_{1/2}$, $4p_{3/2}$, and $4d_{5/2}$ binding energies; a Sommerfeld fs screening parameter reduction to place $4p_{1/2}$ and $4d_{3/2}$; and a high-Z scaling of α_d to Eq. (4). Ionization potentials in square brackets were obtained from semiempirically corrected Dirac-Fock (DF) calculations. (See text for details.)

Z	$p_{1/2}$	$p_{3/2}$	$d_{3/2}$	$d_{5/2}$	IP	Ref.	α_d
29	30 535.302	30 783.686	49 935.200	49 942.057	62 316.6	31,32	5.36
30	48 481.00	49 355.04	96 909.74	96 960.40	144 892.6	33	2.296
31	65 169.5	66 887.3	144 085.5	144 200.2	247 855.00	14,34	1.24
32	81 315.0	84 103.0	190 607.0	190 861.0	368 701.0	31	0.7628
33	97 135.0	101 245.0	236 897.0	237 342.0	505 136.0	35	0.5096
34	112 771.1	118 469.1	282 839.0	283 518.9	659 980.0	36	0.3604
35	128 274.0	135 853.0	328 510.0	329 500.0	831 000.0	14,37,38	0.2656
36	143 697.0	153 475.0	374 060.0	375 350.0	1 015 100.0	21,39	0.2021
37	159 075.0	171 410.0	419 554.0	421 317.0	1 214 900.0	40	0.1576
38	174 445.0	189 714.0	465 155.0	467 425.0	1 430 000.0	41	0.1254
39	189 811.0	208 433.0	510 893.0	513 761.0	1 660 000.0	42	0.1014
40	205 202.0	227 627.0	556 897.0	560 464.0	1 905 500.0	43	(0.0828)
41	220 624.0	247 344.0	603 241.0	607 609.0	2 166 300.0	44	0.069 06
42	236 085.0	267 632.0	649 976.0	655 242.0	2 440 600.0	45	0.057 94
43	(251 652.0)	(288 608.0)	(697 347.0)	(703 672.0)	(2 730 583.0)		(0.0495)
44	267 178.0	310 131.0	744 998.0	752 505.0	3 034 700.0	46	(0.0423)
45	282 831.0	332 369.0	793 345.0	802 134.0	3 355 000.0	46	(0.0364)
46	298 532.0	355 495.0	842 449.0	852 741.0	3 690 000.0	46	(0.0315)
47	314 336.0	379 403.0	892 277.0	904 224.0	4 039 800.0	46	0.027 09
48	330 174.0	404 186.0	942 945.0	956 707.0	4 405 300.0	46	0.0237
49	346 089.0	429 863.0	994 448.0	1 010 283.0	4 785 900.0	46	(0.0210)
50	362 235.0	456 665.0	1 047 076.0	1 065 058.0	5 180 900.0	46	(0.0185)
51	(378 381.0)	(484 375.0)	(1 100 320.0)	(1 120 830.0)	(5 591 096.0)		(0.0164)
52	(394 824.0)	(513 333.0)	(1 155 024.0)	(1 178 224.0)	(6 017 237.0)		(0.0146)
53	411 015.0	543 774.0	1 209 737.0	1 235 815.0	[6 458 600.0]	22	0.012 98
54	427 426.0	574 918.0	1 268 221.0	1 297 520.0	6 912 400.0	47	0.011 64
55	(444 575.0)	(607 737.0)	(1 326 696.0)	(1 359 506.0)	(7 388 562.0)		0.010 46
56	461 060.0	641 970.0	1 386 980.0	1 423 320.0	7 877 000.0	48	0.009 435
57	477 400.0	677 670.0	1 447 800.0	1 488 810.0	8 380 800.0	48	(0.008 50)
58	(494 300.0)	(714 875.0)	(1 511 144.0)	(1 556 204.0)	(8 900 580.0)		(0.007 70)
59	(511 743.0)	(753 760.0)	(1 575 811.0)	(1 625 611.0)	(9 436 192.0)		(0.006 99)
60	529 190.0	794 300.0	1 642 220.0	1 697 010.0	9 988 500.0	48	(0.006 36)
61	(546 698.0)	(836 777.0)	(1 710 383.0)	(1 770 773.0)	(10 555 355.0)		(0.005 80)
62	564 080.0	880 980.0	1 780 520.0	1 846 510.0	11 138 200.0	48	(0.005 30)
63	(581 667.0)	927 394.0	(1 852 759.0)	1 925 319.0	[11 736 000.0]	49	(0.004 86)
64	599 070.0	975 640.0	1 926 820.0	2 005 780.0	12 352 400.0	48	(0.004 46)
65	(616 940.0)	(1 026 375.0)	(2 003 199.0)	(2 089 669.0)	(12 988 550.0)		0.004 138
66	634 820.0	1 079 310.0	2 082 430.0	2 176 260.0	13 644 800.0	48	(0.003 78)
67	(652 704.0)	(1 134 629.0)	(2 163 183.0)	(2 265 483.0)	(14 304 750.0)		(0.003 49)
68	671 420.0	1 193 140.0	2 248 630.0	2 359 180.0	14 990 000.0	48	(0.003 22)
69	(689 312.0)	(1 253 135.0)	(2 333 722.0)	(2453 822.0)	(15 689 109.0)		(0.002 98)
70	708 770.0	1 317 280.0	2 425 060.0	2 554 540.0	16 396 000.0	48	(0.002 77)
71	(726 816.0)	(1 382 997.0)	(2 515 776.0)	(2 656 076.0)	(17 143 187.0)		(0.002 57)
72	(745 781.0)	(1 452 563.0)	(2 611 696.0)	(2 762 896.0)	(17 896 909.0)		(0.002 39)
73	766 700.0	1 526 700.0	2 713 900.0	2 875 700.0	18 669 000.0	48	(0.002 23)
74	787 100.0	1 602 900.0	2 816 800.0	2 990 800.0	19 460 000.0	48	0.002 094
75	(806 300.0)	(1 681 802.0)	(2 920 610.0)	(3 108 610.0)	(20 267 625.0)		(0.001 94)
76	(826 363.0)	(1 765 659.0)	(3 031 399.0)	(3 232 999.0)	(21 095 213.0)		(0.001 81)
77	(846 412.0)	(1 853 553.0)	(3 146 345.0)	3 362 345.0)	(21 941 905.0)		(0.001 70)
78	(866 687.0)	(1 945 682.0)	(3 265 781.0)	(3 496 881.0)	(22 807 962.0)		0.001 598
79	889 007.0	2 043 819.0	3 393 892.0	3 639 912.0	[23 697 500.0]	50	0.001 498
80	(908 354.0)	(2 143 455.0)	(3 518 661.0)	(3 782 461.0)	(24 599 205.0)		0.001 405
81	(929 619.0)	(2 249 509.0)	(3 652 566.0)	(3 933 966.0)	(25 524 889.0)		(0.001 32)
82	952 925.0	2 361 331.0	3 795 369.0	4 092 903.0	[26 472 000.0]	50	0.001 24

TABLE I. (*Continued*).

Z	$p_{1/2}$	$p_{3/2}$	$d_{3/2}$	$d_{5/2}$	IP	Ref.	α_d
83	975 134.0	2 475 615.0	3 935 904.0	4 252 698.0	[27 437 000.0]	50	(0.001 17)
84	(1 000 818.0	(2 598 771.0)	(4 086 430.0)	(4 425 930.0)	(28 424 895.0)		(0.001 10)
85	(1 025 105.0)	(2 726 195.0)	(4 242 227.0	(4 603 027.0)	(29 433 160.0)		(0.001 04)
86	(1 049 251.0)	(2 859 407.0)	(4 403 829.0)	(4 786 929.0)	(30 462 442.0)		9.763*e*-4
87	(1 073 118.0)	(2 998 551.0)	(4 571 334.0)	(4 977 734.0)	(31 512 802.0)		(9.27*e*-4)
88	(1 096 527.0)	(3 143 741.0)	(4 744 692.0)	(5 175 492.0)	(32 584 240.0)		(8.77*e*-4)
89	(1 119 248.0)	(3 295 056.0)	(4 923 899.0)	(5 380 199.0)	(33 676 683.0)		(8.31*e*-4)
90	(1 137 927.0)	3 449 465.0	(5 101 949.0)	5 584 849.0	[34 782 800.0]	50	(7.87*e*-4)
91	(1 161 404.0)	(3 616 148.0)	(5 299 387.0)	(5 810 087.0)	(35 923 849.0)		(7.46*e*-4)
92	(1 182 098.0)	3 787 879.0	(5 495 070.0)	(6 034 870.0)	[37 082 800.0]	50	6.987*e*-4

TABLE II. Theoretical lifetimes for $4p_{1/2,3/2}$ and oscillator strengths for the $4s$-$4p_{1/2,3/2}$ transitions of the Cu isoelectronic sequence.

		Lifetime (ns)		f	
Atom	Z	$4p_{1/2}$	$4p_{3/2}$	s-$p_{1/2}$	s-$p_{3/2}$
Cu	29	7.250 75	7.069 42	0.221 75	0.447 56
Zn	30	2.524 37	2.385 53	0.252 67	0.515 98
Ga	31	1.348 47	1.242 53	0.261 77	0.539 37
Ge	32	0.863 86	0.777 35	0.262 46	0.545 31
As	33	0.607 42	0.533 80	0.261 59	0.547 97
Se	34	0.445 77	0.382 50	0.264 45	0.558 53
Br	35	0.364 96	0.305 35	0.249 65	0.532 05
Kr	36	0.296 53	0.241 76	0.244 84	0.526 52
Rb	37	0.247 75	0.196 57	0.239 13	0.519 15
Sr	38	0.211 25	0.162 92	0.233 21	0.511 33
Y	39	0.182 73	0.136 80	0.227 72	0.504 49
Zr	40	0.160 24	0.116 29	0.222 19	0.497 59
Nb	41	0.142 32	0.099 98	0.216 41	0.490 18
Mo	42	0.127 23	0.086 39	0.211 41	0.484 56
Tc	43	0.114 87	0.075 27	0.206 10	0.478 28
Ru	44	0.104 28	0.065 85	0.201 39	0.473 38
Rh	45	0.095 27	0.057 94	0.196 72	0.468 49
Pd	46	0.087 50	0.051 10	0.192 25	0.464 35
Ag	47	0.080 71	0.045 22	0.187 99	0.460 62
Cd	48	0.074 80	0.040 14	0.183 84	0.457 26
In	49	0.069 63	0.035 74	0.179 77	0.454 07
Sn	50	0.064 88	0.031 82	0.176 10	0.451 88
Sb	51	0.060 71	0.028 41	0.172 49	0.449 86
Te	52	0.057 61	0.027 32	0.166 94	0.416 45
I	53	0.053 45	0.022 71	0.165 74	0.446 91
Xe	54	0.050 50	0.020 31	0.162 49	0.446 58
Cs	55	0.047 58	0.018 21	0.159 42	0.445 70
Ba	56	0.045 11	0.016 33	0.156 33	0.445 61
La	57	0.042 91	0.014 64	0.153 30	0.445 99
Ce	58	0.040 80	0.013 15	0.150 41	0.446 30
Pr	59	0.038 72	0.011 80	0.147 87	0.447 30
Nd	60	0.036 83	0.010 60	0.145 34	0.448 50
Pm	61	0.035 10	0.009 51	0.142 93	0.450 24
Sm	62	0.033 53	0.008 54	0.140 52	0.452 17
Eu	63	0.032 05	0.007 67	0.138 24	0.454 61
Gd	64	0.030 74	0.006 89	0.135 90	0.457 02
Tb	65	0.029 49	0.006 20	0.133 59	0.459 46
Dy	66	0.028 37	0.005 58	0.131 11	0.461 40
Ho	67	0.027 27	0.005 01	0.129 05	0.464 92
Er	68	0.026 16	0.004 49	0.127 12	0.468 70
Tm	69	0.025 22	0.004 04	0.125 10	0.472 45

TABLE II. (*Continued*).

Atom	Z	Lifetime (ns) $4p_{1/2}$	Lifetime (ns) $4p_{3/2}$	f s-$p_{1/2}$	f s-$p_{3/2}$
Yb	70	0.024 16	0.003 62	0.123 55	0.477 54
Lu	71	0.023 38	0.003 26	0.121 40	0.481 01
Hf	72	0.022 53	0.002 93	0.119 61	0.485 70
Ta	73	0.021 59	0.002 62	0.118 15	0.491 05
W	74	0.020 76	0.002 35	0.116 57	0.496 05
Re	75	0.020 07	0.002 11	0.114 90	0.501 40
Os	76	0.019 37	0.001 90	0.113 33	0.507 21
Ir	77	0.018 73	0.001 70	0.111 75	0.513 21
Pt	78	0.018 11	0.001 53	0.110 20	0.519 47
Au	79	0.017 42	0.001 36	0.108 90	0.526 32
Hg	80	0.016 94	0.001 23	0.107 29	0.532 94
Tl	81	0.016 39	0.001 10	0.105 84	0.539 82
Pb	82	0.015 77	0.000 98	0.104 69	0.547 36
Bi	83	0.015 25	0.000 88	0.103 40	0.554 53
Po	84	0.014 60	0.000 79	0.102 49	0.562 75
At	85	0.014 07	0.000 71	0.101 40	0.570 83
Rn	86	0.013 58	0.000 63	0.100 30	0.579 25
Fr	87	0.013 13	0.000 57	0.099 14	0.587 71
Ra	88	0.012 73	0.000 51	0.097 95	0.596 42
Ac	89	0.012 38	0.000 46	0.096 70	0.605 28
Th	90	0.012 17	0.000 41	0.095 15	0.614 00
Pa	91	0.011 83	0.000 37	0.093 96	0.623 45
U	92	0.011 59	0.000 33	0.092 61	0.633 07

TABLE III. Theoretical lifetimes for $4d_{3/2,5/2}$ and oscillator strengths for the $4p_{1/2,3/2}$-$4d_{3/2}$ and $4p_{3/2}$-$4d_{5/2}$ transitions of the Cu isoelectronic sequence.

Atom	Z	Lifetime (ns) $3d_{3/2}$	Lifetime (ns) $3d_{5/2}$	f $p_{1/2}$-$d_{3/2}$	f $p_{3/2}$-$d_{3/2}$	f $p_{3/2}$-$d_{5/2}$
Cu	29	13.008 29	13.111 60	0.511 06	0.052 01	0.467 27
Zn	30	1.362 57	1.388 12	0.784 89	0.079 52	0.714 83
Ga	31	0.443 65	0.456 00	0.909 73	0.091 68	0.825 03
Ge	32	0.218 60	0.226 52	0.964 65	0.096 68	0.871 05
As	33	0.130 61	0.136 40	0.989 27	0.098 69	0.890 09
Se	34	0.086 71	0.091 36	1.008 68	0.100 05	0.903 53
Br	35	0.065 29	0.069 38	0.968 50	0.095 57	0.864 32
Kr	36	0.050 19	0.053 88	0.954 06	0.093 65	0.847 85
Rb	37	0.040 20	0.043 56	0.933 77	0.091 15	0.826 56
Sr	38	0.033 15	0.036 30	0.911 31	0.088 45	0.803 19
Y	39	0.027 92	0.030 91	0.889 44	0.085 80	0.780 40
Zr	40	0.23 93	0.026 81	0.867 09	0.083 11	0.757 21
Nb	41	0.020 83	0.023 63	0.843 99	0.080 35	0.733 39
Mo	42	0.018 29	0.021 01	0.824 20	0.077 92	0.712 52
Tc	43	0.016 22	0.018 89	0.803 60	0.075 42	0.691 05
Ru	44	0.014 48	0.017 11	0.785 51	0.073 15	0.671 69
Rh	45	0.013 02	0.015 62	0.767 61	0.070 92	0.652 59
Pd	46	0.011 76	0.014 33	0.751 19	0.068 81	0.634 72
Ag	47	0.010 67	0.013 21	0.735 91	0.066 82	0.617 87
Cd	48	0.009 72	0.012 24	0.721 48	0.064 90	0.601 72
In	49	0.008 88	0.011 39	0.707 68	0.063 05	0.586 29
Sn	50	0.008 13	0.010 62	0.695 65	0.061 36	0.572 16
Sb	51	0.007 46	0.009 94	0.684 07	0.059 72	0.558 59
Te	52	0.007 05	0.009 51	0.654 22	0.057 22	0.535 10
I	53	0.006 32	0.008 76	0.663 27	0.056 66	0.533 48
Xe	54	0.005 80	0.008 24	0.655 64	0.055 34	0.522 88
Cs	55	0.005 37	0.007 78	0.646 15	0.053 91	0.511 24

TABLE III. (*Continued*).

Atom	Z	Lifetime (ns) $3d_{3/2}$	Lifetime (ns) $3d_{5/2}$	f $p_{1/2}$-$d_{3/2}$	f $p_{3/2}$-$d_{3/2}$	f $p_{3/2}$-$d_{5/2}$
Ba	56	0.004 94	0.007 35	0.639 06	0.052 64	0.500 96
La	57	0.004 57	0.006 96	0.632 17	0.051 38	0.491 30
Ce	58	0.004 22	0.006 59	0.625 92	0.050 20	0.481 82
Pr	59	0.003 90	0.006 25	0.620 26	0.049 09	0.473 14
Nd	60	0.003 61	0.005 94	0.615 11	0.048 01	0.464 81
Pm	61	0.003 34	0.005 64	0.610 80	0.046 99	0.457 13
Sm	62	0.003 08	0.005 36	0.607 21	0.046 03	0.449 72
Eu	63	0.002 85	0.005 10	0.604 24	0.045 11	0.443 07
Gd	64	0.002 63	0.004 86	0.601 42	0.044 19	0.436 18
Tb	65	0.002 43	0.004 63	0.598 35	0.043 26	0.429 42
Dy	66	0.002 25	0.004 43	0.594 26	0.042 26	0.421 74
Ho	67	0.002 08	0.004 22	0.593 03	0.041 46	0.416 29
Er	68	0.001 92	0.004 02	0.592 39	0.040 72	0.411 03
Tm	69	0.001 77	0.003 85	0.591 43	0.039 93	0.405 73
Yb	70	0.001 63	0.003 66	0.592 74	0.039 33	0.401 95
Lu	71	0.001 51	0.003 50	0.591 25	0.038 50	0.396 21
Hf	72	0.001 39	0.003 34	0.591 84	0.037 83	0.391 84
Ta	73	0.001 27	0.003 19	0.593 30	0.037 24	0.387 97
W	74	0.001 17	0.003 04	0.594 14	0.036 60	0.383 95
Re	75	0.001 08	0.002 91	0.595 26	0.035 94	0.380 15
Os	76	0.000 99	0.002 77	0.597 40	0.035 36	0.376 74
Ir	77	0.000 91	0.002 65	0.599 85	0.034 79	0.373 47
Pt	78	0.000 84	0.002 52	0.602 68	0.034 25	0.370 41
Au	79	0.000 76	0.002 40	0.606 44	0.033 79	0.367 87
Hg	80	0.000 70	0.002 29	0.609 50	0.033 22	0.364 96
Tl	80	0.000 64	0.002 19	0.613 13	0.032 71	0.362 35
Pb	82	0.000 59	0.002 08	0.617 94	0.032 31	0.360 19
Bi	83	0.000 54	0.001 99	0.621 50	0.031 80	0.357 53
Po	84	0.000 49	0.001 89	0.625 90	0.031 34	0.355 96
At	85	0.000 45	0.001 80	0.630 74	0.030 90	0.354 08
Rn	86	0.000 41	0.001 72	0.636 08	0.030 48	0.352 40
Fr	87	0.000 38	0.001 64	0.641 57	0.030 06	0.350 72
Ra	88	0.000 34	0.001 56	0.647 43	0.029 65	0.349 17
Ac	89	0.000 31	0.001 49	0.653 61	0.029 24	0.347 68
Th	90	0.000 28	0.001 43	0.659 56	0.028 77	0.345 65
Pa	91	0.000 26	0.001 36	0.666 87	0.028 43	0.344 85
U	92	0.000 24	0.001 30	0.673 61	0.027 98	0.343 13

through U^{63+}, and its quantum defect can be predicted by interpolation alone. For the $4d\,^2D_{5/2}$ energy, extrapolation was necessary only from Th^{61+} through U^{63+}, and all other ions were obtained by interpolation.

A semilogarithmic plot of quantum defects for the $4s_{1/2}$, $4p_{3/2}$, and $4d_{5/2}$ levels versus nuclear charge for the Cu sequence is shown in Fig. 2. The interpolation was achieved by a weighted least-squares fit of the logarithm of the quantum defect to a low-order polynomial in the ionization stage $\zeta = Z - 28$, including only data with $Z \geq 42$. The weights were obtained from the uncertainties quoted in the source references,[21,31–48] and the optimum order of the polynomial was chosen to be five by use of the chi-squared probability test. The fitted values are indicated in Fig. 2 by solid lines, and the observed data are denoted by solid circles. The complete data set is given in Table I, with source references indicated for measured values, theoretical ionization potentials enclosed in brackets, and semiempirical interpolations and extrapolations enclosed in parentheses. No attempt has been made to truncate significant figures with zeros, but comparisons with measured data indicate that the semiempirical estimates are reliable to within parts in 10^4.

The transition matrix elements calculated here [cf. Eq. (3)] also require specification of the dipole polarizability of the Ni-like core of the Cu sequence. Calculations for this quantity using the relativistic random-phase approximation (RRPA) have been made by Johnson *et al.*[54] for 27 selected ions in this sequence, and we have interpolated these values using the empirically fitted screening parametrization:

$$\alpha_d = a/(Z-b)^c \tag{4}$$

in the region $Z \geq 40$ (a reasonable fit was obtained from $a \cong 7300$, $b \cong 19.5$, $c = 3.77$). These values are also listed in Table II, with the interpolations enclosed in parentheses.

TABLE IV. Comparison of the available ANDC-type and cascade-free $4p\ ^2P$ and $4d\ ^2D$ lifetime measurements with the present and other calculations for the Cu isoelectronic sequence.

		Experiment		Theory	
Ion	Level	ANDC	Other	Present	DF[a]
Cu I	$4p\ ^2P_{1/2}$		7.5(3)[b]	7.251	
	$4p\ ^2P_{3/2}$		7.3(1)[b]	7.069	
	$4d\ ^2D_{3/2}$		11(2)[c]	13.008	
	$4d\ ^2D_{5/2}$			13.112	
Zn II	$4p\ ^2P_{1/2}$			2.524	
	$4p\ ^2P_{3/2}$	2.07(20)[d]	2.4(3)[e]	2.386	
	$4d\ ^2D_{3/2}$			1.363	
	$4d\ ^2D_{5/2}$		1.40(15)[d]	1.388	
Ga III	$4p\ ^2P_{1/2}$		1.2(2)[f]	1.350	
	$4p\ ^2P_{3/2}$	1.22(10)[f]		1.244	
	$4d\ ^2D_{3/2}$	0.35(15)[f]		0.444	
	$4d\ ^2D_{5/2}$	0.42(08)[f]		0.456	
Ge IV	$4p\ ^2P_{1/2}$	0.91(5)[g]		0.864	0.758
	$4p\ ^2P_{3/2}$	0.82(5)[g]		0.777	0.685
	$4d\ ^2D_{3/2}$		0.25(4)[g]	0.219	
	$4d\ ^2D_{5/2}$		0.31(5)[g]	0.227	
As V	$4p\ ^2P_{1/2}$	0.68(9)[h]		0.607	0.539
	$4p\ ^2P_{3/2}$	0.54(3)[h]		0.534	0.476
	$4d\ ^2D_{3/2}$		0.166(12)[h]	0.131	
	$4d\ ^2D_{5/2}$		0.18(2)[h]	0.136	
Se VI	$4p\ ^2P_{1/2}$	0.45(5)[i]		0.460	0.408
	$4p\ ^2P_{3/2}$	0.39(4)[i]		0.395	0.352
	$4d\ ^2D_{3/2}$		0.11(2)[i]	0.087	
	$4d\ ^2D_{5/2}$		0.14(3)[i]	0.091	
Kr VIII	$4p\ ^2P_{1/2}$	0.291(12)[j] 0.290(15)[k]		0.297	0.265
	$4p\ ^2P_{3/2}$	0.243(10)[j] 0.218(33)[k]		0.242	0.217
Mo XIV	$4p\ ^2P_{1/2}$		0.118(8)[l]	0.127	0.116
	$4p\ ^2P_{3/2}$		0.079(6)[l]	0.086	0.079
I XXIV	$4p\ ^2P_{1/2}$	0.0467(20)[m]		0.0535	
	$4p\ ^2P_{3/2}$	0.0231(10)[m]		0.0227	
	$4d\ ^2D_{3/2}$		0.0114(10)[m]	0.0063	
	$4d\ ^2D_{5/2}$		0.0098(9)[m]	0.0088	

[a]Reference 8.
[b]Reference 25.
[c]Reference 55.
[d]Reference 15.
[e]Reference 24.
[f]Reference 16.
[g]Reference 17
[h]Reference 18.
[i]Reference 19.
[j]Reference 20.
[k]Reference 21.
[l]Reference 23.
[m]Reference 22.

V. RESULTS

Our calculations for lifetimes and oscillator strengths for the $n=4$ levels are presented in Tables II and III and compared with critically selected experimental results in Tables IV and V. Table IV presents the $4p$ and $4d$ lifetimes and selects primarily ANDC measurements for presentation. The agreement between computation and measurement is to within experimental uncertainties. For the $4d$ levels, ANDC measurements have been made only for Ga III (Ref. 13), and their agreement with the present calculations is excellent. The other $4d$ results cited[15,17–19,22,55] were obtained by simple curve-fitting methods, and the tendency of some of these lifetime measurements to exceed the theoretical predictions is almost certainly a result of unaccounted cascade repopulation in the experimental decay curves. ANDC analyses incorporating the $4d$-$4f$ (and possibly other) decay curves into the $4p$-$4d$ analysis could elucidate this problem.

The single-configuration Dirac-Fock (DF) calculations of Cheng and Kim,[8] also shown in Table IV, give systematically shorter lifetimes than our values and are in

TABLE V. Experimental and theoretical oscillator strengths for $4s\ ^2S$–$4p\ ^2P$ transitions in the Cu isoelectronic sequence.

Ion	Upper level	Experiment ANDC	Theory Present	Theory Other	NCA[a]
Cu I	$4p\ ^2P_{1/2}$		0.2218	0.215[b]	0.2631
	$4p\ ^2P_{3/2}$		0.4476	0.434[b]	0.5296
	multiplet		0.6694	0.649[b]	0.7827
				0.624[c]	
Zn II	$4p\ ^2P_{1/2}$		0.2527	0.238[b]	0.2965
	$4p\ ^2P_{3/2}$	0.513(60)[d]	0.5160	0.487[b]	0.6046
	multiplet	0.768(90)[d]	0.7687	0.724[b]	0.9011
				0.732[c]	
Ga III	$4p\ ^2P_{1/2}$		0.2614	0.246[b]	0.2973
	$4p\ ^2P_{3/2}$	0.549(45)[e]	0.5386	0.508[b]	0.6114
	multiplet	0.843(5)[e]	0.8000	0.752[b]	0.9087
				0.792[c]	
Ge IV	$4p\ ^2P_{1/2}$	0.249(14)[f]	0.2625	0.247[b]	0.2918
	$4p\ ^2P_{3/2}$	0.517(32)[f]	0.5453	0.513[b]	0.6050
	multiplet	0.77(5)[f]	0.8078	0.759[b]	0.8968
As V	$4p\ ^2P_{1/2}$	0.233(20)[g]	0.2616	0.254[b]	0.2855
	$4p\ ^2P_{3/2}$	0.542(40)[g]	0.5480	0.532[b]	0.5969
	multilet	0.78(6)[g]	0.8096	0.786[b]	0.8824
				0.802[c]	
Se VI	$4p\ ^2P_{1/2}$	0.262(30)[h]	0.2560	0.243[b]	0.2758
	$4p\ ^2P_{3/2}$	0.548(60)[h]	0.5409	0.513[b]	0.5816
	multiplet	0.83(9)[h]	0.7969	0.756[b]	0.8574
				0.624[c]	
Kr VIII	$4p\ ^2P_{1/2}$	0.25(1)[i]	0.2448	0.220[b]	0.2578
	$4p\ ^2P_{3/2}$	0.53(2)[i]	0.5265	0.473[b]	0.5537
	multiplet	0.78(3)[i]	0.7713	0.693[b]	0.8115
				0.771[c]	
Mo XIV	$4p\ ^2P_{1/2}$	0.23(2)[j]	0.2114	0.190[b]	0.2192
	$4p\ ^2P_{3/2}$	0.53(4)[j]	0.4846	0.437[b]	0.5024
	multiplet	0.76(6)[j]	0.6960	0.627[b]	0.7216
				0.706[c]	
I XXV	$4p\ ^2P_{1/2}$	0.190(8)[k]	0.1657		
	$4p\ ^2P_{3/2}$	0.439(19)[k]	0.4469		
	multiplet	0.629(27)[k]	0.6126		
Xe XXVI	$4p\ ^2P_{1/2}$		0.1625	0.172[l]	
	$4p\ ^2P_{3/2}$		0.4466	0.473[l]	
	multiplet		0.6091	0.644[l]	
				0.679[c]	
W XLVI	multiplet		0.6126	0.665[c]	

[a]Reference 14
[b]Reference 12, relativistic model potential with core polarization.
[c]Reference 10.
[d]Reference 15.
[e]Reference 16.
[f]Reference 17.
[g]Reference 18.
[h]Reference 19.
[i]Reference 20.
[j]Reference 23.
[k]Reference 22.
[l]Reference 12, relativistic Hartree Fock.

the opposite direction from the experimental trend. We discuss this behavior further below within the context of oscillator strengths.

Table V compares the present results for 4s-4p absorption oscillator strengths with those obtained by inverting measured 4p lifetimes, as well as the DF calculations of Cheng and Kim[8] and Migdalek and Baylis which included core polarization effects,[9] the multiconfiguration Hartree-Fock (MCHF) calculations of Froese Fischer[10] which included both core-polarization and correlation effects, and the numerical Coulomb approximation (NCA) results of Lindgård *et al.*[14] Figure 3 presents a plot of the individual line and multiplet absorption oscillator strengths versus $1/Z$.

Our values are in agreement with all the experimental values to within quoted error limits, with the exception of

TABLE VI. Comparison of core polarization parameters.

Spectrum	α_d Present	α_d (Ref. 12)	r_c	r_0 (Ref. 12) $4s$	$4p_{1/2}$	$4p_{3/2}$
Cu I	5.360	6.21	2.537	0.996	0.903	0.896
Zn II	2.296	2.81	2.109	0.872	0.859	0.857
Ga III	1.240	1.58	1.850	0.783	0.783	0.783
Ge IV	0.7628	0.938	1.661	0.715	0.715	0.715
As V	0.5096	0.540	1.523	0.661	0.661	0.661
Se VI	0.3604	0.433	1.410	0.615	0.615	0.615
Br VII	0.2656	0.365	1.314	0.576	0.576	0.548
Kr VIII	0.2021	0.307	1.241	0.542	0.542	0.542
Mo XIV	0.057 94	0.100	0.924	0.423	0.423	0.423

the $4p_{1/2}$ to I XXV. This is also the case for the multiplet values of the MCHF calculation.[10] Our values are in excellent agreement with those of Ref. 10, essentially because both approaches account for the same major effect, i.e., core polarization by the valence electron. The MCHF method includes it through a multiconfiguration treatment, whereas our method introduces it through the effective core polarizability α_d. The discussion at the end of Sec. III, however, indicates that the MCHF results will worsen beyond Mo XIV, since it then becomes necessary to use different radial wave functions for $4p_{1/2}$ and $4p_{3/2}$.

Our values are also in reasonable agreement with the calculations of Migdalek and Baylis[12] who performed relativistic Hartree-Fock and relativistic model-potential calculations incorporating the core-polarization effect through a polarization potential of the form

$$V_p = -\tfrac{1}{2}\alpha_d r^2 (r^2 + r_0^2)^{-3} , \tag{5}$$

and a corrected dipole matrix element

$$\langle f|r|i\rangle \rightarrow \langle f|r[1-\alpha_d (r^2+r_0^2)^{-3/2}]|i\rangle , \tag{6}$$

instead of the one used here [cf. Eq. (3)]. Theodosiou[26] made some comparison calculations and analyses of these two types of implementation of the core-polarization effects in terms of the appropriate cutoff values r_c and r_0. The differences between the results of our calculations and those of Ref. 12 are due to three factors: (a) we used different cutoff forms as just discussed, (b) we used, presumably, more accurate dipole polarizability values α_d, and (c) we used nonadjustable cutoff distances r_c. We believe that most of the differences result from part (b) above. Mo XIV is the most extreme case where the difference between the α_d values used in the two works differs by almost a factor of 2. Table VI compares our values of α_d and cutoff radii with those of Ref. 12.

Our work has common features with that of Lindgård *et al.*,[14] which used a numerical Coulomb approximation with an inward integration and an adjustable small-r cutoff. That work, however, did not account for core-polarization effects that lower the transition probability values. Their f values are therefore higher than ours, as should be expected.

As was already demonstrated for the alkali-metal atoms,[26] He I (Refs. 56 and 57), Li II (Ref. 58), Cu II (Ref. 59), Ag II (Ref. 59), and the Na isoelectronic sequence,[27] the present approach yields accurate oscillator strengths and lifetimes, at least in the cases where Rydberg series are not perturbed. It is our hope that the results of this work will stimulate further accurate experimental investigations, especially at high ionicity.

ACKNOWLEDGMENTS

We are grateful to Dr. Nina Reistad for providing us with her Ph.D. thesis, which comprehensively analyzes the empirical systematics of lifetimes in the Cu I sequence. The work of L.J.C. was supported by the Division of Chemical Sciences, Office of Basic Energy Sciences, U.S. Department of Energy, under Contract No. DE-AS05-80ER10676.

[1] R. J. S. Crossley, L. J. Curtis, and C. Froese Fischer, Phys. Lett. **57A**, 220 (1976).
[2] S. M. Younger and W. L. Wiese, Phys. Rev. A **18**, 2366 (1978).
[3] L. J. Curtis, H. G. Berry, and J. Bromander, Phys. Lett. **34A**, 169 (1971).
[4] L. J. Curtis, in *Beam-Foil Spectroscopy*, edited by S. Bashkin (Springer-Verlag, Berlin, 1976), pp. 63–109.
[5] L. Engström, Nucl. Instrum. Methods **202**, 369 (1982).
[6] K. Weckström, Phys. Scr. **23**, 849 (1981).
[7] E. H. Pinnington and R. N. Gosselin, J. Phys. (Paris) Colloq. **40**, CI-149 (1979).
[8] K.-T. Cheng and Y.-K. Kim, At. Data Nucl. Data Tables **22**, 547 (1978).
[9] K.-T. Cheng and R. A. Wagner, Phys. Rev. A **36**, 5435 (1987).
[10] C. Froese Fischer, J. Phys. B **10**, 1241 (1977).
[11] A. W. Weiss, J. Quant. Spectrosc. Radiat. Transfer **18**, 481 (1977).
[12] J. Migdalek and W. E. Baylis, J. Phys. B **12**, 1113 (1979).
[13] S. M. Younger, Phys. Rev. A **20**, 951 (1979).
[14] A. Lindgård, L. J. Curtis, I. Martinson, and S. E. Nielsen, Phys. Scr. **21**, 47 (1980).
[15] I. Martinson, L. J. Curtis, S. Huldt, U. Litzén, L. Liljeby, S. Mannervik, and B. Jelenkovic, Phys. Scr. **19**, 17 (1979).
[16] W. Ansbacher, E. H. Pinnington, J. L. Bahr, and J. A. Kernahan, Can. J. Phys. **63**, 1330 (1985).
[17] E. H. Pinnington, J. L. Bahr, and D. J. G. Irwin, Phys. Lett.

84A, 247 (1981).
[18]E. H. Pinnington, J. L. Bahr, J. A. Kernahan, and D. J. G. Irwin, J. Phys. B **14**, 1291 (1981).
[19]J. L. Bahr, E. H. Pinnington, J. A. Kernahan, and J. A. O'Neill, Can. J. Phys. **60**, 1108 (1982).
[20]E. H. Pinnington, R. N. Gosselin, J. A. O'Neill, J. A. Kernahan, K. E. Donnelly, and R. L. Brooks, Phys. Scr. **20**, 151 (1979).
[21]A. E. Livingston, L. J. Curtis, R. M. Schectman, and H. G. Berry, Phys. Rev. A **21**, 771 (1980).
[22]B. M. Johnson, K. W. Jones, D. C. Gregory, J. O. Ekberg, L. Engström, T. H. Kruse, and J. L. Cecchi, Phys. Scr. **32**, 210 (1985).
[23]B. Denne and O. Poulsen, Phys. Rev. A **23**, 1229 (1981).
[24]F. H. K. Rambow and L. D. Shearer, Phys. Rev. A **14**, 1735 (1976).
[25]P. Hannaford and D. C. McDonald, J. Phys. B **11**, 1177 (1978).
[26]C. E. Theodosiou, Phys. Rev. A **30**, 2881 (1984).
[27]C. E. Theodosiou and L. J. Curtis, Phys. Rev. A **38**, 4435 (1988).
[28]D. R. Bates and A. Damgaard, Philos. Trans. R. Soc. London, Ser. A **242**, 101 (1949).
[29]I. B. Bersuker,Opt. Spektrosk. **3**, 97 (1957).
[30]S. Hameed, A. Herzenberg, and M. G. James, J. Phys. B **1**, 822 (1968).
[31]C. E. Moore, *Atomic Energy Levels*, Natl. Bur. Stand. (U.S.) Circ. No. 467 (U.S. GPO, Washington, D.C., 1952), Vol. II.
[32]G. Tondello, J. Opt. Soc. Am. **63**, 346 (1973).
[33]W. C. Martin and V. Kaufman, J. Res. Natl. Bur. Stand. **74A**, 11 (1970).
[34]Y. N. Joshi, K. S. Bhatia, and W. E. Jones, Spectrochim. Acta **28B**, 149 (1973).
[35]R. A. Sawyer and C. J. Humphreys, Phys. Rev. **32**, 583 (1928).
[36]Y. N. Joshi and Th. A. M. van Kleef, Physica **94C**, 270 (1978).
[37]A. S. Rao and K. R. Rao, Proc. Phys. Soc. (London) **46**, 163 (1934).
[38]A. E. Livingston and S. J. Hinterlong, Phys. Rev. A **23**, 758 (1981).
[39]B. C. Fawcett, B. B. Jones, and R. Wilson, Proc. Phys. Soc. (London) **78**, 1223 (1961).
[40]S. Goldsmith, J. Reader, and N. Acquista, J. Opt. Soc. Am. B **1**, 631 (1984).
[41]N. Acquista and J. Reader, J. Opt. Soc. Am. **71**, 569 (1981).
[42]J. Reader and N. Acquista, J. Opt. Soc. Am. **69**, 1285 (1979).
[43]J. Reader and N. Acquista, J. Opt. Soc. Am. **69**, 1659 (1979).
[44]J. Reader and N. Acquista, J. Opt. Soc. Am. **70**, 317 (1980).
[45]J. Reader, G. Luther, and N. Acquista, J. Opt. Soc. Am. **69**, 144 (1979).
[46]J. Reader, N. Acquista, and D. Cooper, J. Opt. Soc. Am. **73**, 1765 (1983).
[47]V. Kaufman, J. Sugar, and W. L. Rowan, J. Opt. Soc. Am. **5**, 1273 (1988).
[48]J. Reader and G. Luther, Phys. Scr. **24**, 732 (1981).
[49]G. A. Doschek, U. Feldman, C. M. Brown, J. F. Seely, J. O. Ekberg, W. E. Behring, and M. C. Richardson, J. Opt. Soc. Am. B **5**, 243 (1988).
[50]J. F. Seely, J. O. Ekberg, C. M. Brown, U. Feldman, W. E. Behring, J. Reader, and M. C. Richardson, Phys. Rev. Lett. **57**, 2924 (1986).
[51]I. P. Grant, B. J. McKenzie, P. H. Norrington, D. F. Mayers, and N. C. Pyper, Comput. Phys. Commun. **21**, 207 (1980).
[52]L. J. Curtis, J. Phys. B **14**, 631 (1981).
[53]L. J. Curtis, Phys. Rev. A **35**, 2089 (1987).
[54]W. R. Johnson, D. Kolb, and K.-N. Huang, At. Data Nucl. Data Tables **28**, 333 (1983).
[55]L. J. Curtis, B. Engman, and I. Martinson, Phys. Scr. **13**, 109 (1976).
[56]C. E. Theodosiou, Phys. Rev. A **30**, 2910 (1984).
[57]C. E. Theodosiou, At. Data Nucl. Data Tables **36**, 97 (1987).
[58]C. E. Theodosiou, Phys. Scr. **32**, 129 (1985).
[59]C. E. Theodosiou, J. Opt. Soc. Am. B **3**, 1107 (1986).